Modelling and feedback control of turbulent coherent structures for bluff body drag reduction

Rowan D. Brackston

Dept. Aeronautics, Imperial College London
London, SW7 2AZ, United Kingdom
r.brackston13@imperial.ac.uk

Andrew Wynn

Dept. Aeronautics, Imperial College London
London, SW7 2AZ, United Kingdom
a.wynn@imperial.ac.uk

Juan Marcos García de la Cruz

Dept. Aeronautics, Imperial College London
London, SW7 2AZ, United Kingdom
juanm.garcial04@imperial.ac.uk

Jonathan F. Morrison

Dept. Aeronautics, Imperial College London
London, SW7 2AZ, United Kingdom
j.morrison@imperial.ac.uk

ABSTRACT

Three-dimensional bluff body wakes are of key importance due to their relevance to the automotive industry. Such wakes have both large pressure drag and a number of coherent flow structures associated with them. Depending on the geometry, these structures may include both a bistability resulting from a reflectional symmetry breaking (RSB), and a quasi-periodic vortex shedding. The authors have recently shown that the bistability may be modelled by a Langevin equation and that this model enables the design of a feedback control strategy that efficiently reduces the drag through suppression of asymmetry. In this work the modelling approach is extended to the vortex shedding, capturing both the forced and unforced behaviour. A control strategy is then presented that makes use of the frequency response of the wake, and aims to reduce the measured fluctuations associated with the vortex shedding. The strategy proves to be effective at suppressing fluctuations within specific frequency ranges but, due to amplification of disturbances at other frequencies, is unable to give drag reduction.

INTRODUCTION

The flow over three-dimensional bluff bodies is of particular interest due to its relevance to automotive vehicles. Such bodies experience large pressure drag due to the large region of separated flow in the wake. For automotive vehicles operating at motorway speeds, this pressure drag is responsible for a significant proportion of the fuel consumption, therefore its reduction is a topic of key interest.

Three-dimensional bluff body wakes exhibit a number of key coherent structures, two of which are the static asymmetry and the quasi-oscillatory vortex shedding. Both features arise initially at very low Reynolds numbers (Re) as respectively a reflectional symmetry breaking (RSB) mode (Grandemange *et al.*, 2012), and a temporal symmetry breaking, yet both are also observed at the much higher Reynolds numbers typical of road vehicles. In the flows over rectilinear bluff bodies, the RSB mode is observed as an instantaneous asymmetry, mainly appearing in the recirculation region as displayed in figure 1(a). Under aligned flow conditions the wake flips randomly between two asymmetric states, each mirror symmetric with respect to the other, a phenomenon known as wake bistability. The instantaneous asymmetry of the wake leads to a lateral force and contributes to the pressure drag on the body. The feature is quite general, having been observed for a range of three-dimensional bluff bodies of widely varying geometries (Rigas *et al.*, 2015). Superposed on this, the vortex shedding is seen as quasi-periodic oscillations of the wake, occuring in both the lateral and the vertical dimensions (Grandemange *et al.*, 2013; Volpe *et al.*, 2015). The relative importance of these two features with respect to the pressure drag on the body remains unclear.

The objective of this research is to develop efficient drag reduction methods for three-dimensional bluff bodies, without making large geometric modifications. A promising method for doing this involves suppression of coherent structures, including the RSB mode and vortex shedding. Some passive methods such as a control cylinder in the wake (Cadot *et al.*, 2015) or a base cavity (Evrard *et al.*, 2015) have already shown promising results for both the suppression of the asymmetry and pressure drag reduction. However while effective, such passive methods may involve large geometric modifications and the exact requirements for suppression of the coherent structures remains unclear. This motivates a careful analysis of the physics of coherent structures in the wake, and the use of active feedback control for their suppression. In this work we develop stochastic models to describe the coherent structures before making use of these models in feedback control design. We will recap some of the recent work of Brackston *et al.* (2016) for the modelling and control of bistability, and extend the approach to the vortex shedding.

EXPERIMENTAL SETUP

Investigations and feedback control are implemented experimentally on a scaled down, flat-back Ahmed body (Ahmed *et al.*, 1984) of the proportions used in many other studies (Grandemange *et al.*, 2012; Cadot *et al.*, 2015), giving Re of $O(10^5)$. This experimental setup is shown in figure 1(b). A force balance measures the total force and moment acting on the body while 8 Endevco 8507C pressure transducers take fluctuating pressure measurements, and an ESP-DTC pressure scanner supplies 64 static pressure measurements distributed over the model base. Forcing of the wake is achieved using two flaps located at the trailing edges of the body, each 19 mm in stream-wise length and running the length of the edges to which they are mounted. The flaps may be positioned either on the lateral edges for control of the bistability and lateral shedding, or on the top and bottom edges for control of the vertical shedding. The flaps are mounted on hinges and driven by internal motors that regulate their motion. The angle of each flap (θ) is measured using a 12 bit magnetic encoder while the power supplied to the flaps is monitored through measurement of the supply voltage and current.

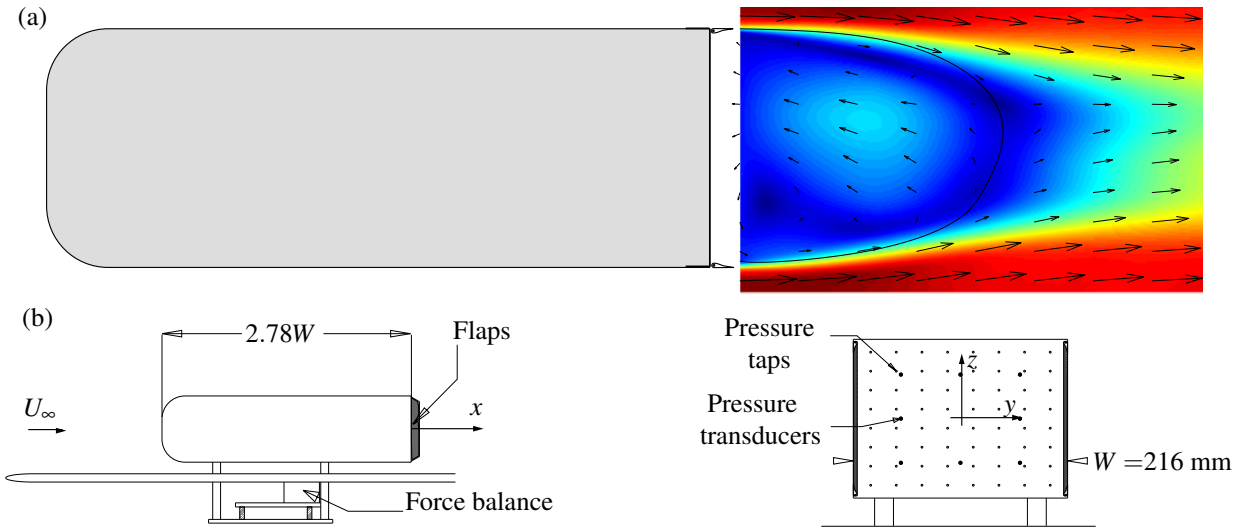

Figure 1. Plan view of the experiment including an average example of the bistable feature of the wake (a), and the overall assembly and detailed view of the base (b).

STOCHASTIC MODELLING OF COHERENT STRUCTURES

A first step in the understanding and control of coherent structures in a turbulent flow, is the development of low-order models for their dynamics. Such models may give insight into the nature of feedback control strategies that may then be applied. A promising approach is based upon the observation that these coherent structures in the turbulent flow are often the persistence of the bifurcations seen at very low *Re* (Rigas *et al.*, 2014). This allows the development of phenomenological models that make use of the equations governing these low *Re* bifurcations, with the addition of stochastic terms to model the effect of turbulent fluctuations. We will discuss below the application of such an approach to the modelling of the RSB mode and the vortex shedding.

Bistability

For the Ahmed body of this experiment, the RSB mode gives a bistable wake in the lateral dimension. This feature of the wake may be quantified in terms of a metric r, defined as the lateral (y) location of the center of pressure on the model base:

$$r(t) = \int yp(y,t)\mathrm{d}A \Big/ \int p(y,t)\mathrm{d}A. \qquad (1)$$

Applying the stochastic modelling approach, we may write an equation for the RSB mode of the wake, quantified by r, as the equation governing a pitchfork bifurcation with the addition of a stochastic forcing. Additionally the influence of the flaps is included via a term $b\theta_{t-\tau}$, capturing the linear influence of the flaps and incorporating an advective time delay τ:

$$\dot{r} = \alpha r - \lambda r^3 + b\theta_{t-\tau} + \sigma\xi(t). \qquad (2)$$

As detailed in Brackston *et al.* (2016), the parameters from this model may be found be examining the probability distribution (PDF) of the metric r as well as the frequency response between θ and r. Given the model of (2), the steady-state PDF for r is given by a Fokker-Planck equation which may be shown to be written as:

$$P(r) = C\exp\left(\frac{\alpha}{\sigma^2}\left(r^2 - \frac{1}{2}\frac{\lambda}{\alpha}r^4\right) + \frac{2b\theta}{\sigma^2}r\right), \qquad (3)$$

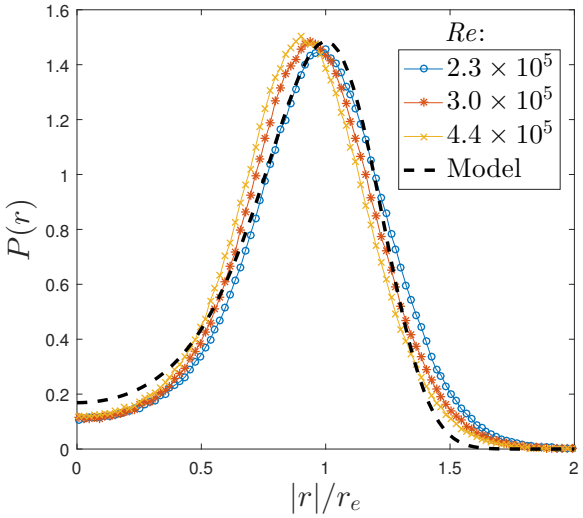

Figure 2. Unforced PDF for the metric r for three different *Re* along with the fit from the Fokker-Planck equation of (3).

where C is a normalisation constant. By comparing this analytical distribution with the experimental data the ratios σ^2/α and λ/α may be determined. The time-scales defined by α and τ may then be found from the frequency response.

The PDF of the unforced wake is displayed for a limited range of *Re* in figure 2. Also displayed is the fit from the Fokker-Planck equation, demonstrating the good agreement that may be obtained under unforced conditions for which $\theta = 0$.

It is also important to note that the model accurately captures the forced response of the wake. Through static offsets the flaps can induce the wake to remain in one or other of the two asymmetric states, an effect that may again be described by the Fokker-Planck equation with non-zero θ. Under harmonic forcing the flaps induce repeated flipping of the wake between these two states. Under such forcing the measured response acts something like a 1st-order low-pass filter with a large response at low frequencies that reduces as the forcing frequency increases above α.

Vortex Shedding

The stochastic modelling approach may also be extended to the vortex shedding in the wake. In this case the initial bifurcation is a Hopf bifurcation, leading to limit cycle behaviour and described by a complex Stuart-Landau equation. The shedding may therefore be modelled by such an equation with the addition of a stochastic forcing term:

$$\dot{\boldsymbol{x}} = \boldsymbol{\alpha}\boldsymbol{x} - \boldsymbol{\lambda}\boldsymbol{x}|\boldsymbol{x}|^2 + \boldsymbol{u}(\theta) + \boldsymbol{\sigma}\xi(t), \tag{4}$$

where all bold symbols denote complex quantities. A complex Stuart-Landau equation such as this is known to be capable of modelling self-excited oscillations (Li & Juniper, 2013), and will generate limit-cycle behaviour with a fixed frequency ω_0 under unforced conditions (i.e. $\theta = 0$). The unique addition here is to include the stochastic term, just as for the bistability modelling, the effect of which is to spread the frequency content around ω_0. This generates the broadband oscillations observed for vortex shedding in turbulent flows. A simulated time-series and power spectral density for the imaginary part of $\boldsymbol{x}$ are displayed in figure 3. The results demonstrate the broadband oscillations that the model generates, demonstrating that the model may qualitatively capture the vortex shedding behaviour observed in many turbulent wake flows.

In addition to the unforced response, of key interest for feedback control is the response of the model in (4) to forcing, quantified by the frequency response. Applying a purely real $u_r(t) = U\sin(\omega t)$, and taking as output the imaginary part of $\boldsymbol{x}$, we may evaluate the frequency response displayed in figure 4. The simulated results here demonstrate that despite the cubic nonlinearity present in the underlying equations, the input-output behaviour may be captured accurately by the frequency response of a linear 2nd-order oscillator.

We may compare the simulated results from (4) with experimental data for the harmonically forced wake. The experimental frequency response for several forcing amplitudes is displayed in figure 5. The interaction of the flaps with the vortex shedding in the wake is seen for $St_H \approx 0.2$, at which the amplitude of the response is seen to reach a maximum, indicative of a resonance of the vortex shedding. Coinciding with this resonance is a decrease of the phase angle from -2π to around -3π. This coincidence of a peak in the amplitude and $-\pi$ shift in the phase is just as observed for the simulated results displayed in figure 4.

Frequency Response Interpretation

The models described above give nonlinear stochastic equations for the dynamics of the bistability caused by the RSB mode and the quasi-oscillatory vortex shedding. Despite the nonlinearity of the underlying models and flow, it is important to note that we can still deduce linear input-output behaviour in the form of the frequency response. We may therefore hope to explain fully the features of the experimental frequency response of figure 5, based upon the models for the flow.

One significant feature of the experimental frequency response is the sharp trough in $|G|$ and the accompanying phase shift seen at $St_H \approx 0.09$. This behaviour is indicative of what are known as right-half-plane zeros in control theory, and can result from a cancellation between two independent sets of dynamics, dominant over different frequency ranges. Such a pair of dynamics may indeed result from the combined ability of forcing flaps to alter both the orientation of the separation bubble at low frequencies, and interact with the oscillatory vortex shedding at higher frequencies. As discussed above, we may expect the frequency response of each of these features to behave like 1st and 2nd-order linear systems, giving the following transfer functions:

$$G_1(s) = g_1 \frac{1}{1+sT_1} = \frac{n_1}{d_1}, \tag{5}$$

$$G_2(s) = g_2 \frac{1}{1+2\zeta sT_2 + s^2T_2^2} = \frac{n_2}{d_2}. \tag{6}$$

In order for a cancellation to occur, the two transfer functions must be added together, $G = G_1 + G_2$. This is based on the idea that the two features are essentially independent, therefore the total response of the wake may be considered as the sum of the two responses. The poles of the resulting transfer function G will be the poles of the two constituent transfer functions, however the zeros will not be the same but are instead given by the roots of

$$\begin{aligned} n(s) &= g_1\left(1+2\zeta sT_2+s^2T_2^2\right) + g_2(1+sT_1) \\ &= g_1+g_2+(2g_1\zeta T_2+g_2T_1)s+g_1T_2^2s^2 \\ &= g\left(1+2\zeta_z T_z s+T_z^2 s^2\right). \end{aligned} \tag{7}$$

The criteria for the pair of RHP zeros observed experimentally are therefore,

$$g_1 + g_2 = g > 0, \tag{8a}$$

$$2g_1\zeta T_2 + g_2T_1 = 2g\zeta_z T_z < 0, \tag{8b}$$

$$g_1T_2^2 = gT_z^2 > 0. \tag{8c}$$

These criteria may be satisfied by appropriate choice of the parameters, and furthermore the properties of the response may be chosen to fit with observations. For example, if we specify the DC gain g, the properties of the zeros (specified by T_z and ζ_z) and the properties of the poles (specified by ζ and T_2), we have enough information to determine all remaining parameters. The black line displayed in figure 5 is just such a fit composed of the sum of 1st and 2nd-order linear systems. This fit can be seen to capture the key behaviour in both magnitude and phase.

While the data displayed in figure 5 is for the case of vertical forcing, the frequency response for lateral forcing exhibits the same key features. In both cases, the dynamics of the wake may therefore be considered to consist of the sum of low-frequency reorientation of the separation bubble, either through continuous deflection or flipping between bistable configurations, and high-frequency interaction with the vortex shedding.

FEEDBACK CONTROL

Given the modelling and our understanding of the wake features, feedback control may proceed along one of two approaches. Either the static asymmetry of the wake may be targeted, aiming to achieve a more symmetric wake on average, or we may target the unsteadiness associated with vortex shedding. The former of these strategies will be applied in the lateral dimension in which the bistability is present, while the latter will be applied in the vertical dimension in which the interaction of the flaps and shedding is stronger. A schematic of the block diagram that applies for both cases is displayed in figure 6. In this schematic the wake is modelled as the sum of two transfer functions, G_1 capturing the response

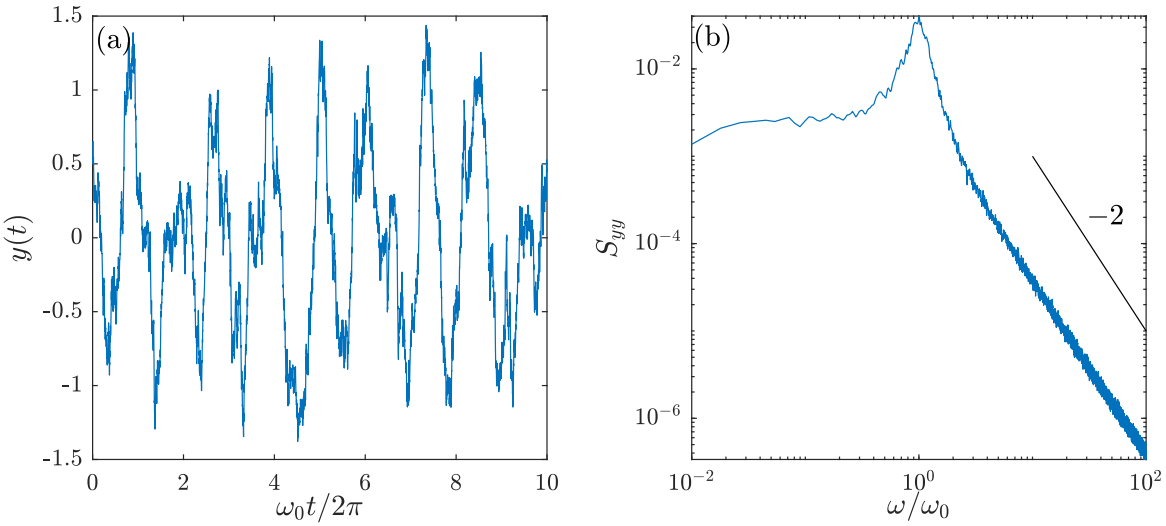

Figure 3. Unforced time series (left) and power spectral density (right) for the variable $y = a\sin(\psi)$ of (4).

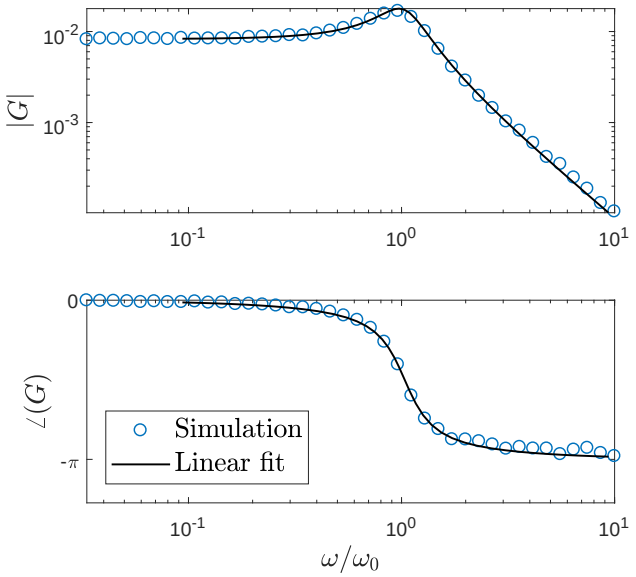

Figure 4. Frequency response of the model (4) between real input $u_r = U\sin(\omega t)$ and imaginary output x_i. Also shown is a linear 2nd-order fit to the data.

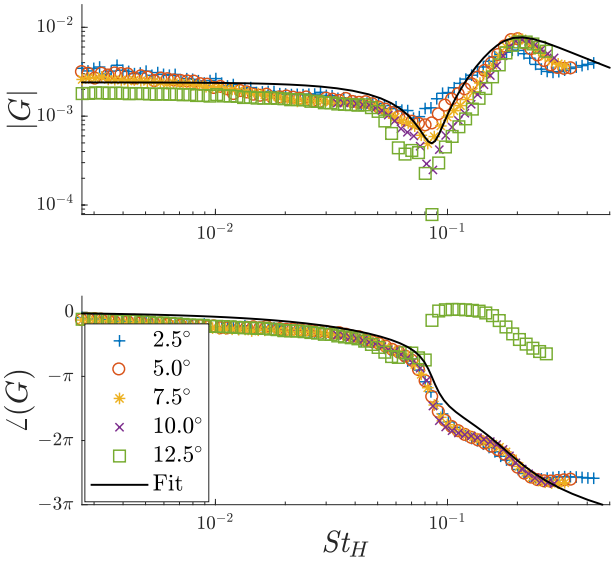

Figure 5. Experimental frequency response between forcing with the top/bottom flaps and the vertical pressure gradient m_v. For comparison the composite model evaluated as the sum $G_1(s)+G_2(s)$ is also shown.

of the low-frequency behaviour of the bistability or static wake deflection and G_2 capturing the interaction of the flaps with the vortex shedding. The disturbances d describe all other unmodelled dynamics entering the measurement m. The transfer function A describes the dynamics of the actuators while K is the feedback controller.

Bistability

Feedback control of the bistability in the wake may be motivated by the model of (2), which suggests that the RSB mode has an unstable equilibrium at $r = 0$, corresponding to a symmetric wake. The model of (2) may be linearised and put into a form suitable for control design as:

$$G_1(s) = \frac{\bar{r}(s)}{\bar{\theta}(s)} = \frac{b(2/\tau - s)}{(s-\alpha)(2/\tau + s)}, \qquad (9)$$

It may be shown (Brackston *et al.*, 2016) that a suitable proportional feedback is sufficient to stabilise this system, implying a more symmetric wake. In practise however, care must be taken to take into account the interaction between the flaps and wake at higher frequencies, as described by G_2. The results of such a control strategy are demonstrated in figure 7, which shows the probability distribution of the pressure metric r and the power spectral density, both with and without control. The results demonstrate that effective control may render the flow much more symmetric on average, but that additional fluctuations are generated at higher frequencies of around $St_W \approx 0.15$. These fluctuations provide a limitation to the efficacy of the control in providing a drag reduction. A maximum drag reduction of 2% is obtained via this strategy which, although modest, is energetically efficient as the power consumed by the flaps is only 24% of that saved through drag reduction.

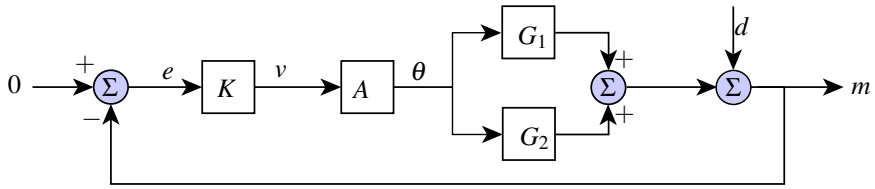

Figure 6. A schematic of the feedback control loop comprising the wake $G_{1,2}$, actuator A and feedback controller K. G_1 captures the low-frequency dynamics of the bistability (lateral) or near-wake deflection (vertical), while G_2 captures the vortex shedding and shear layer dynamics at higher frequencies.

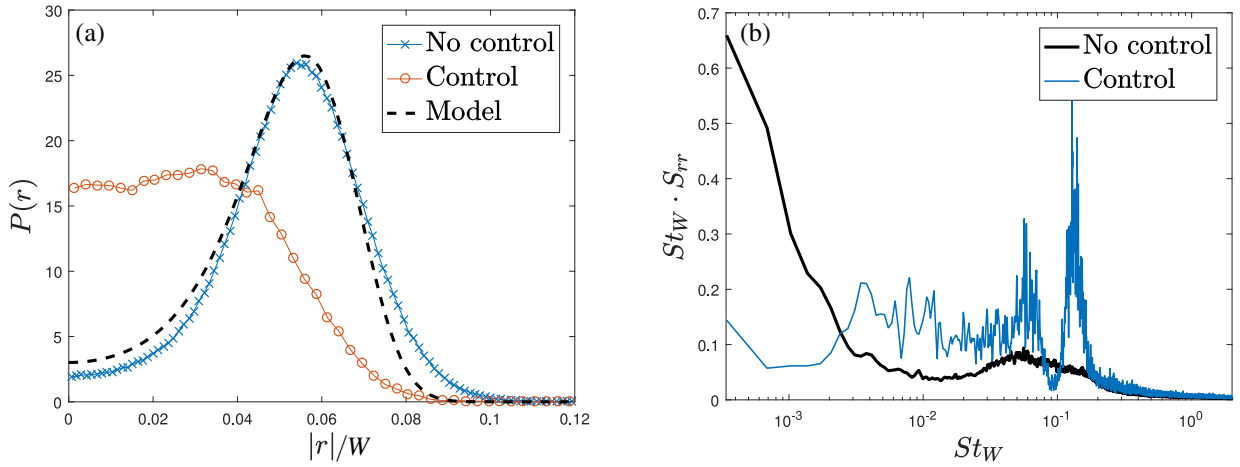

Figure 7. Comparison of the natural and controlled flow: (a) the PDF and (b) the power spectrum for r.

Vortex Shedding

The alternative control strategy is to target fluctuations directly, specifically aiming to reduce the fluctuations at $St \approx 0.2$ associated with the vortex shedding. To do this we may design controllers based on the sensitivity function $S(\omega)$. This is an approach that has been successfully applied before in fluid flows (Dahan *et al.*, 2012), and may be based purely upon empirical linear models of the input-output behaviour. In this case we therefore do not seek to linearise (4), but rather make use of the frequency response characteristics discussed above and displayed in figure 5. For the application of this approach using the top/bottom flaps G_1 is a simple 1st-order low-pass filter while G_2 is a second order oscillator, chosen to fit the frequency response in figure 5. The pressure measurement m is ytaken as the vertical pressure gradient on the base of the body.

For the feedback-control configuration displayed in figure 6 the sensitivity function is defined as:

$$S(\omega) = \frac{1}{1+(G_1+G_2)AK}. \qquad (10)$$

This is the transfer function from disturbances d to the measurement m, and therefore gives the ratio of the measured fluctuations with and without feedback control. For frequencies at which $S(\omega) > 1$ fluctuations will be amplified while for those at which $S(\omega) < 1$, they will be suppressed. Through control design methods such as $\mathscr{H}_\infty$ loop-shaping, we may design controllers that have $S(\omega) < 1$ over particular frequency ranges such as $St \approx 0.2$.

A total of 123 controllers were tested, each giving a slightly different $S(\omega)$. Each controller therefore provided amplification and attenuation of measured fluctuations over slightly different frequency ranges. Despite the large number of variations trialled, none of the controllers were able to give a measurable drag reduction and, moreover, most gave a drag increase. The PSD from once such controller is displayed in figure 8. The comparison between the controlled and uncontrolled spectra demonstrate that the controller has suppressed measured fluctuations in the frequency range around $St_H \approx 0.2$, although it has significantly amplified fluctuations at other frequencies. This is much the same issue that was found for the case of bistability control and it is likely that these additional fluctuations lead to the drag increase. Unfortunately, in both cases some amplification is essential due to the waterbed effect and furthermore, is restricted in frequency by the presence of the right-half-plane zeros in the frequency response (see for example Skogestad & Postlethwaite, 2005). Given that none of the controllers proved successful at drag reduction, it is difficult to determine whether the fluctuation suppression has any beneficial effect, or if it is simply offset by the impact of amplification at other frequencies.

CONCLUDING REMARKS

We have presented a stochastic modelling approach suitable for two of the coherent structures observed in three-dimensional bluff body wakes: the RSB mode and the vortex shedding. This approach takes the equation describing the underlying bifurcation observed at low Re, and adds a stochastic term to model phenomenologically the effect of turbulent fluctuations on the large-scale coherent structures.

Given the modelling and our understanding of the forced response of the flow using dynamic flaps, we have presented two feedback-control design approaches. For the first of these, the stochastic model for the bistability of the flow may be linearised directly, motivating a controller that has a suitable DC gain. Such control aims to symmetrise the wake, changing the quasi-static behaviour. Provided that the interaction with the higher frequency dynamics is also taken into account, such control may give drag reductions of up to 2% and in an energetically efficient manner. This is in agreement with results from other authors who have demon-

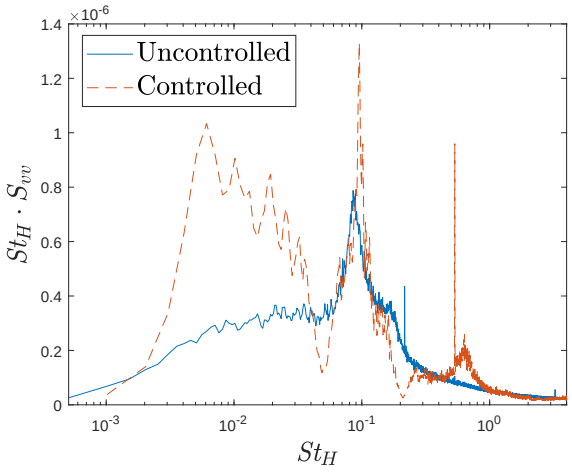

Figure 8. PSD of the vertical pressure gradient m_v for a particular controller. Suppression is achieved around $St_H \approx 0.2$, however the drag is not reduced.

strated feedback control of bistability with similar levels of drag reduction (Li *et al.*, 2016). There is scope for improvement on these feedback controllers if strategies can be achieved that minimise the amplification of other fluctuations in the wake, as these additional fluctuations are generally detrimental to the drag reduction.

The second feedback-control approach is one that targets the measured fluctuations in the wake rather than the static behaviour. This control approach may take advantage of the linear frequency response implied by the nonlinear stochastic models, in order to design controllers based upon the sensitivity function. We have demonstrated that measured fluctuations of the vertical pressure gradient may be suppressed over the frequency range of the vortex shedding, although no controllers were found that could give a resultant drag reduction. The success may again be limited by the amplification of measured fluctuations over other frequency ranges, and to some extent is the result of fundamental limitations in the application of linear control. It would be interesting to see if nonlinear approaches could get around these issues and provide improved drag reduction in the future.

REFERENCES

Ahmed, S., Ramm, G. & Faltin, G. 1984 Some salient features of the time-averaged ground vehicle wake. *SAE Tech. Rep.* **840300**, Society of Automotive Engineers.

Brackston, R. D., García de la Cruz, J. M., Wynn, A., Rigas, G. & Morrison, J. F. 2016 Stochastic modelling and feedback control of bistability in a turbulent bluff body wake. *J. Fluid Mech.* **802**, 726–749.

Cadot, O., Evrard, A. & Pastur, L. 2015 Imperfect supercritical bifurcation in a three-dimensional turbulent wake. *Phys. Rev. E* **91**, 063005.

Dahan, J. A., Morgans, A. S. & Lardeau, S. 2012 Feedback control for form-drag reduction on a bluff body with a blunt trailing edge. *J. Fluid Mech.* **704**, 360–387.

Evrard, A., Cadot, O., Herbert, V., Ricot, D., Vigneron, R. & Délery, J. 2015 Fluid force and symmetry breaking modes of a 3D bluff body with a base cavity. *J. Fluid Struct.* **61**, 99–114.

Grandemange, M., Cadot, O. & Gohlke, M. 2012 Reflectional symmetry breaking of the separated flow over three-dimensional bluff bodies. *Phys. Rev. E* **86**, 035302.

Grandemange, M., Gohlke, M. & Cadot, O. 2013 Turbulent wake past a three-dimensional blunt body. Part 1. Global modes and bi-stability. *J. Fluid Mech.* **722**, 51–84.

Li, L. K. B. & Juniper, M. P. 2013 Lock-in and quasiperiodicity in a forced hydrodynamically self-excited jet. *J. Fluid Mech.* **726**, 624–655.

Li, R., Barros, D., Borée, J., Cadot, O., Noack, B. R. & Cordier, L. 2016 Feedback control of bimodal wake dynamics. *Exp. Fluids* **57**, 158.

Rigas, G., Morgans, A. S., Brackston, R. D. & Morrison, J. F. 2015 Diffusive dynamics and stochastic models of turbulent axisymmetric wakes. *J. Fluid Mech.* **778**, R2.

Rigas, G., Oxlade, A. R., Morgans, A. S. & Morrison, J. F. 2014 Low-dimensional dynamics of a turbulent axisymmetric wake. *J. Fluid Mech.* **755**, R5.

Skogestad, S. & Postlethwaite, I. 2005 *Multivariable Feedback Control. Analysis and Design*, 2nd edn. John Wiley & Sons Inc.

Volpe, R., Devinant, P. & Kourta, A. 2015 Experimental characterization of the unsteady natural wake of the full-scale square back Ahmed body: flow bi-stability and spectral analysis. *Exp. Fluids* **56**, 99.